A Fourier Transform Spectrometer based on Birefringent Interferometer

Chu-Yu Huang[1,3], Wei-Chih Wang[1,2,4]*

[1]*Department of Mechanical Engineering, University of Washington, Seattle, Washington 98195, USA*
[2]*Department of Electrical Engineering, University of Washington, Seattle, Washington 98195, USA*
[3]*Electronics and Optoelectronics Research Laboratories, Industrial Technology Research Institute, Hsinchu, Taiwan*
[4]*Medical Device innovation Center, National Cheng Kung University, Tainan, Taiwan*
**Corresponding author: abong@u.washington.edu*

Abstract— **A simple Fourier transform spectrometer design without moving parts is presented. The compact and rugged design utilizes a birefringent prism, a pair of polarizers and a linear CCD array to achieve this spectrometer design. The advantages of this design over existing FTIR systems are: 1) No moving parts. Therefore these designs are not sensitive to vibration. 2) Much more compact and portable. 3) No scanning is invovled. Instead of timely varying the optical path difference, the optical path difference is spread out spatially, which dramatically reduce the measuring time. In this paper, theoretical models and experimental results are presented. The optical performance of the model is tested using several LEDs of known wavelengths. Fringe counting technique is employed in the interferogram acquisition process to ensure accurate sampling of the interferogram at constant optical path difference intervals. The reconstructed spectra yielded detected wavelengths which deviated by less than 1 nm from the actual wavelengths.**

Keywords- Fourier transform spectrometer, birefringent interferometer, spectrometer

I. INTRODUCTION

Since first portable Fourier transform spectrometer (FTS) being sold by Digilab in 1969, further developments in computer technology, together with substantial price decreases, have been responsible for the large number of commercial FT-IR spectrometers on the market and for the wide application of FT-IR spectroscopy in all branches of science and technology [1]. Currently, there are many commercially available FTS, primarily used in the lab applications that provide high resolution. To achieve appropriate resolution levels, these Fourier transform spectrometers require a scanning mirror mechanism with high precision control necessitating a large size, heavy weight and high cost for the equipment. Their size and mass makes them ill-suited to on-site chemical analysis, such as measurement of oxygen levels in the sap of trees, monitoring the quality of the gasoline at the gas station or blood analysis in third world countries. In fact, there are so many out-of-the lab applications which do not need high resolution FTS, such as, environmental monitoring [2], industrial process control [3], color measurements, and medical diagnostics [4]. Without the requirement of high resolution (typical <1 cm^{-1} or 0.0025nm at wavelength 500nm), the portability and system cost are the primary considerations in selecting a FTS. However, there is no commercially available compact and low cost FTS system suitable for these on-site chemical and biological analysis applications. Therefore, there is a need to make FTS systems smaller and less expensive, further expanding the number and variety of potential applications.

In recent years, a number of attempts have been made to develop compact FTS system [5-8]. Manzardo has developed a lamellar grating based FTS using MEMS technology with a resolution of 5.5 nm at 800 nm [5]. A Micromachined Translatory Actuator based FTS with a maximum resolution of 25 cm^{-1} was presented by Kenda [6]. Solf has developed a miniature FTS with a resolution of 24.5 nm at 1545 nm using LIGA technology [7]. A magnetic actuated polymer is integrated with lamellar grating based FTS with a maximum resolution of 20cm^{-1} was developed by Ataman [8].These systems are mainly using MEMS technology to create a movable micro-actuator to create the interferometers. However, the surface of the microfabricated sidewall is not very smooth and the sidewall thickness is limited, it loses most of light intensity when illuminating on the thin and long mirror area. Additionally, the moving part is always sensitive to vibration which makes the device not best suit for a portable device.

To create a system without moving part, we propose a compact birefringent prism based FTS. This new system has several advantages over previous FTS systems: First, it requires fewer optical components (e.g. lenses, mirrors and beam splitters), allowing for more compact and portable designs. Second, the optical path difference (OPD) is supplied by a prism, where the OPD is controlled by the size of the prism and the resolution of the detector array.

II. THEORY

The schematic of the single birefringent prism based FTS design is illustrated in Figure 1(a). A collimated light beam is input from the left side of the Quartz birefringent prism (uniaxial birefringent material, birefringence Δn =0.00913, right angle prism). A polarizer is used so that the light is polarized at 45° with respect to the vertical direction (shown in Figure 1(b)). The collimated beam enters normally into the left side of the prism, and travels along the optical axis direction of the birefringent prism until it reaches the inclined end of the prism. The light then bounces off the incline surface and make a 90° turn due to the total internal reflection. The light then travels along the direction normal to the optical axis of the prism until it reaches the output end of the prism. An analyzer, placed at the output end of the prism (top side) with the polarization at 45° with respect to the vertical direction, recombines the two polarization of light. The linear CCD array (2048 pixel, Sony ILX511) is placed right next to the analyzer to record the interferogram.

When the light first enter the prism, it travels along the optical axis of the birefringent prism, where there is no optical path

978-1-4673-2877-7/12/$31.00 ©2012 IEEE

difference between the vertical and horizontal polarization of light (because quartz is uniaxial birefringent material). However, once the light is bounced off the incline surface and make a 90° turn due to the total internal reflection, the light travelling direction has shifted and is now normal to the optical axis of the birefringent prism, where there is now an optical path difference between the vertical and horizontal polarization of light. Furthermore, due to the geometry of the birefringent prism; the optical path difference at the output end of the prism (top side) varies across the section (along the x axis). The optical path difference is proportional to the distance y when light traveling in direction normal to the optical axis of the prism. Since the prism is a right angle prism, the distance y at the position x is equal to x. Therefore, the relationship between optical path difference (*OPD)* and the position x can then be expressed as follow:

$$OPD(x) = x \cdot \Delta n \qquad 0 \le x \le L \qquad (1)$$

Where Δn is birefringence of the prism and x is the distance from right edge to the point x.

As the distance increase from 0 to L, the OPD increases linearly from 0 to $L\Delta n$. The vertical and horizontal polarization component of light recombined pass through the analyzer. The resulting interference pattern appear across the linear CCD array due to the OPD between two polarization of light varies across the output side of the prism. The linear CCD array records the interferogram. The interferogram is then converted into a light spectrum by performing a Fourier transformation.

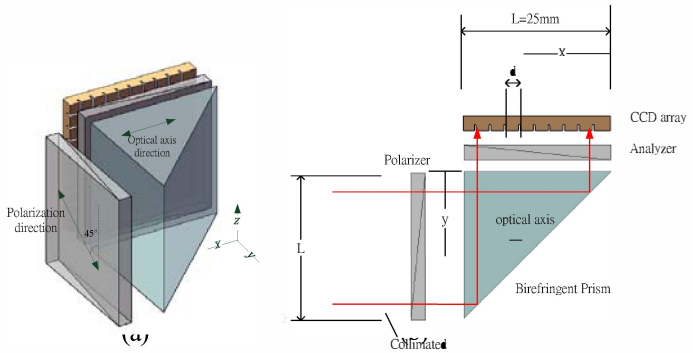

Fig. 1. (a) The schematic of the proposed birefringent prism based FTS design, (b) the polarization direction is at 45° with respect to the vertical direction.

The polarized light propagating though the birefringent prism experiences a phase difference $\Delta\phi(x)$ between the ordinary and extraordinary components of the propagating light. This phase difference $\Delta\phi(x)$ is

$$\Delta\phi(x) = \frac{2\pi x \Delta n}{\lambda} \qquad (2)$$

Here, x is the distance from right edge to the position x (see Figure 1(a)) and λ is the wavelength of the propagating light. In this case, the birefringent prism acts like a linear variable phase shifter with a phase shift change linearly across the side of the prism.

Suppose the input is a monochromatic light of wavelength λ and the intensity of input beam is I_0. The intensity $I(x)$ at the output of the interferometer is:

$$I(x) = \frac{1}{2}\left[I_0 + I_0 \cos(\frac{2\pi x \Delta n}{\lambda}) \right] \qquad (3)$$

The interferogram $F(x)$ which is the variable part of the output intensity $I(x)$ can be expressed as:

$$F(x) = I_0 \cos(2\pi x \sigma) \qquad (4)$$

Where $\sigma = 1/\lambda$ is the wave number. From Eq. (4) we can see that a monochromatic light leads to a cosinusoidal interferogram at the output of the birefringent prism.

The detected interferogram $F(x)$ as a function of x, can be converted into $P(\sigma)$, the intensity spectrum as a function of wave number by a simple Fourier transform (Eq.(5)) [9].

$$P(\sigma) = \frac{2}{\pi}\int_0^L F(x)\cos(2\pi x\sigma)dx \qquad (5)$$

According to the Nyquist–Shannon sampling theorem [10], an analog signal that has been sampled can be perfectly reconstructed from the samples if the sampling rate exceeds 2B samples per second, where B is the highest frequency in the original signal. Nyquist–Shannon sampling theorem suggests that the linear CCD array used to sample the interferogram at the output of the birefringent prism needs to have sufficient resolution. The signal can suffer from aliasing if the sampling resolution, or pixel density, is inadequate. In another word, the highest frequency (or the shortest wavelength) can be resolved is limited by the linear CCD array resolution (pixel density). This limitation can be easily resolved by placing lens in front of the linear CCD array to magnify the interferogram.

The total number of cosinusoidal cycles n_c, when the input is a monochromatic light of wavelength λ, can be expressed as:

$$n_c = \frac{L\Delta n}{\lambda} \qquad (6)$$

Therefore the cosinusoidal cycle density is:

$$\frac{n_c}{L} = \frac{\Delta n}{\lambda} \qquad (7)$$

To perfectly resolve the light of wavelength λ from the samples, the linear CCD array resolution (pixel density) needs to be larger than:

$$\text{Linear CCD pixel density} > \frac{2\Delta n}{\lambda} \qquad (8)$$

III. Experimental Results

Several tests were performed on the Single Birefringent prism based FTS system with different light sources. The experimental setup is shown in Figure 1. A pinhole is used in this setup to create a point source at the focal point of the convex lens. The input light is then collimated by the convex lens and input from one side of the right angle Quartz birefringent prism. The light beam travels inside the birefringent prism and outputs from another side of the prism. The output beam goes through another polarizer again and reaches a linear CCD array (Sony ILX511, 2048 pixels, pixel

pitch= 14 μm). The interferogram is recorded by the linear CCD array.

The first light source used in this experiment is a HeNe laser (wavelength λ = 632.8 nm). Due to the phase difference between the light travels in the ordinary and extraordinary directions, an interferogram of transmitted light was observed. The result is shown in Figure 2. From the figure, we can see that the interferogram recorded by the CCD array packed the space across the linear CCD array, and the intensity is oscillating with a constant frequency. The total number of cosinusoidal cycles, n_c observed from the figure is equal to 352, which is very close to the theoretical number 360.7. The maximum $OPD = n_c$ x λ achieved by this birefringent prism FTS is 222.75 μm . Finally, the optical spectrum the light source (HeNe laser) can be easily calculated from Figure 3 by doing a Fourier transform. Result is shown in Figure 4. The resolution of the result optical spectrum is equal to $0.5\lambda^2 / OPD_{max}$, which is about 1 nm (FWHM). The Figure shows there is a strong intensity peak around 633 nm, which is consistent with our HeNe laser light source. The above results indicate that the proposed birefringent prism FTS works, and the result is consistent with the theoretical model in previous section

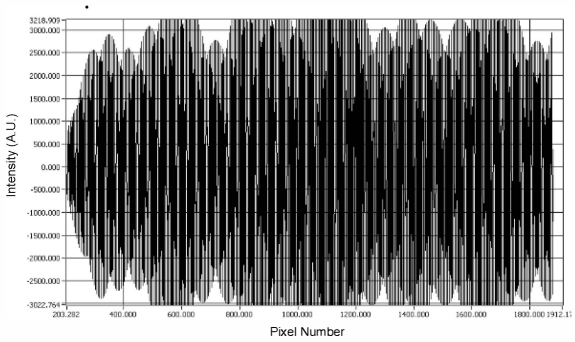

Figure 2: The interferogram observed by linear CCD array

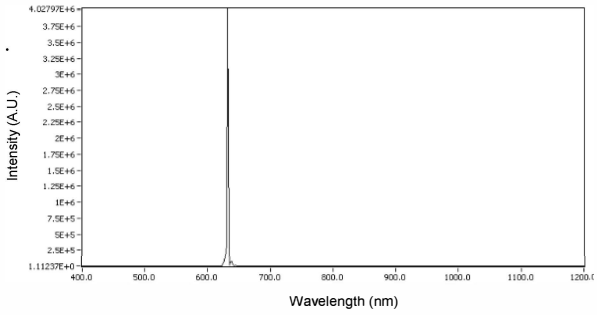

Figure 3: The result spectrum of the HeNe laser.

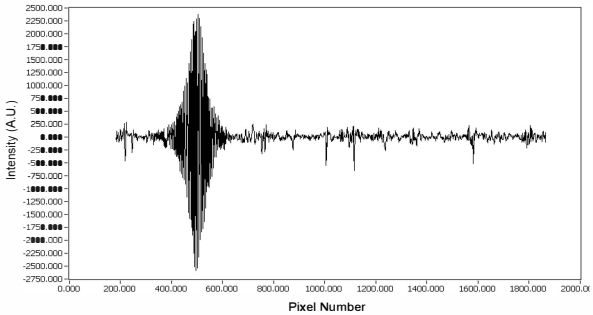

Figure 4: The resulting interferogram for the red LED source.

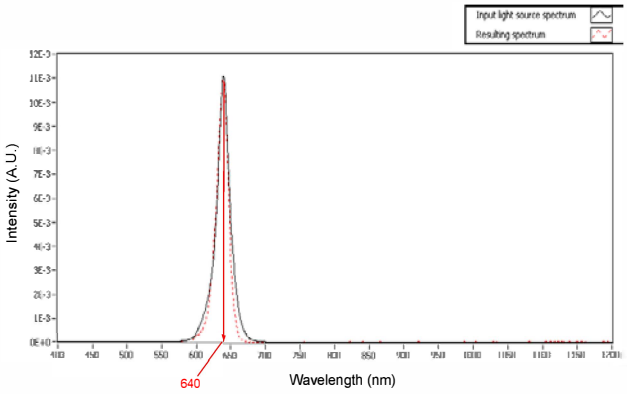

Figure 5: The resulting spectrum for the red LED source.

The second light source used in this experiment is a light-emitting diode (LED, from superbrightled.com, part number: RL5-R12008) with a center wavelength at 640nm. Again, the LED was placed in front of the pinhole at the focal point of the convex lens. The collimated and polarized beam travels inside the prism and output goes through another polarizer. The resulting interferogram (Figure 4) shows the typical broadband interferogram characteristics, high intensity at zero optical path difference position, decade quickly away from zero optical path difference position. Finally, the optical spectrum the light source (LED) was calculated from Figure 4 by doing a Fourier transform. The resulting spectrum is plotted together with the spectrum measured from a commercial spectrometer (Ando AQ6310, resolution = 0.2 nm) in Figure 5. The resulting spectrum shows the center wavelength is at 640 nm, which is consistent with the spectrum measured from the commercial spectrometer

The birefringent prism FTS experiment is repeated seven more times with different LEDs (with center wavelengths at 940nm, 890nm, 640nm, 616nm, 593nm, 516nm, and 462nm separately, part numbers: RL5-IR2730, RL5-IR2730, RL5-R12008, RL5-O5015, RL5-Y10008, RL5-G13008, and RL5-B5515 respectively). Finally, the optical spectra of the light sources (LEDs) were calculated by using Fourier transform. The resulting spectra of these LEDs are plotted together with the spectra measured from a commercial spectrometer in 6. The resulting spectra show that the center wavelength positions are consistent with the spectra measured from the commercial spectrometer.

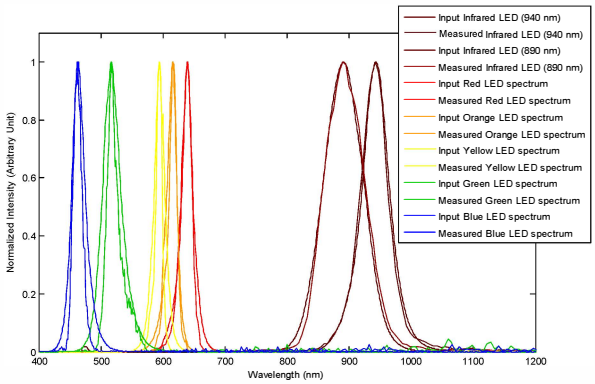

Figure 6: The resulting spectra of five different LEDs.

IV. CONCLUSION

In conclusion, the birefringent prism based FTS is presented in this study. Theoretical models, numerical simulations and experimental results of this FTS design have been demonstrated. According to the experimental results, the birefringent prism based FTS works successfully. A spectral resolution of 1nm with different LEDs (with center wavelengths at 940nm, 890nm, 640nm, 616nm, 593nm, 516nm, and 462nm has been achieved.

References

1. B. C. Smith, Fundamentals of Fourier transform infrared spectroscopy (CRC Press, 1996).
2. U. F. Rodriguez-Zuniga, D. M. B. P. Milori, Da Silva, Wilson Tadeu Lopes, L. Martin-Neto, L. C. Oliveira, and J. C. Rocha, Environmental Science and Technology 42, 1948-1953 (2008).
3. J. Cornel, C. Lindenberg, and M. Mazzotti, Industrial and Engineering Chemistry Research 47, 4870-4882 (2008).
4. F. Severcan, N. Kaptan, and B. Turan, Spectroscopy 17, 569-577 (2003).
5. O. Manzardo, R. Michaely, F. Schadelin, W. Noell, T. Overstolz, N. De Rooij, and H. P. Herzig, Opt. Lett. **29,** 1437-9 (2004).
6. A. Kenda, C. Drabe, H. Schenk, A. Frank, M. Lenzhofer, and W. Scherf, *MEMS, MOEMS, and Micromachining II,* Anonymous (SPIE - The International Society for Optical Engineering, 2006), pp. 618609 (11 pp.).
7. C. Solf, J. Mohr, and U. Wallrabe, *Proceedings of IEEE Sensors 2003,* Anonymous (IEEE, 2003), pp. 773-6.
8. Ç. Ataman and H. Urey, Sensors and Actuators A: Physical **151,** 9-16 (2009).
9. P. R. Griffiths and J. A. De Haseth, Fourier transform infrared spectrometry (Wiley, 1986).
10. C. E. Shannon, Proceedings of the IEEE. **86,** 447 (1998).